



Article

Spatiotemporal Variations and Causes of Wind/Rainfall Erosion Climatic Erosivity in Qinghai Province, China

Yihua Liu ¹, Ge Gao ^{2,*}, Hongmei Li ¹, Lüliu Liu ² , Zong Fan ³ and Tingting Wen ¹¹ Climate Center of Qinghai, Xining 810001, China² National Climate Center, China Meteorological Administration, Beijing 100081, China³ Provincial Geomatics Center of Qinghai, Xining 810001, China

* Correspondence: gage@cma.gov.cn

Abstract: Wind and rainfall climatic erosivities are important parameters with which to assess the possible effects of climatic conditions on erosion. In this study, wind erosion climatic erosivity (C-factor) and rainfall erosivity (R_{day} -factor) were calculated for the period 1970–2020 based on data from 50 meteorological stations in Qinghai Province. The Mann–Kendall test, trend analysis, and K-means clustering method were used to explore the spatiotemporal characteristics of regional wind/rainfall climatic erosivity. Results showed that the annual mean value of the C-factor was 25.8 over the past 51 years, with an obvious trend of decline of 6.5/10a. The mean annual value of the R_{day} -factor was 491.6 MJ·mm/(hm²·h·a), with an obvious trend of increasing of 24.0 MJ·mm/(hm²·h·10a). Strong seasonality was found in both the C-factor and the R_{day} -factor. The highest values of the C-factor were found in late winter and spring, accounting for a substantial proportion of the annual C-factor (48.6%). Rainfall erosivity occurred mainly April–October, with the highest values in summer, accounting for a substantial proportion of the annual R_{day} -factor (72.9%). Wind-erosion climatic erosivity and rainfall erosivity were obviously asynchronous on an annual basis, and the period of their combination extended the time of soil erosion. Through k-means clustering analysis, climatic erosivity in Qinghai Province was divided into three regions: the first dominated by wind-erosion climatic erosivity, the second dominated by rainfall erosivity, and the third dominated by their combination. The most serious land erosion occurred in the third region, accounting for 34.3% of the entire land area of Qinghai Province, where annual rainfall was found to be broadly consistent at 300–400 mm. Wind speed, temperature, rainfall, and sunshine duration are key factors known to impact the variation in wind-erosion climatic erosivity, while annual erosive rainfall, number of rainy days, and sunshine duration are the main factors known to impact the variation in rainfall erosivity. The findings of this study represent a robust reference for ecoenvironmental protection, sustainable development, and soil protection.



Citation: Liu, Y.; Gao, G.; Li, H.; Liu, L.; Fan, Z.; Wen, T. Spatiotemporal Variations and Causes of Wind/Rainfall Erosion Climatic Erosivity in Qinghai Province, China. *Atmosphere* **2022**, *13*, 1649. <https://doi.org/10.3390/atmos13101649>

Academic Editor: Tin Lukic

Received: 23 August 2022

Accepted: 1 October 2022

Published: 10 October 2022

Publisher's Note: MDPI stays neutral with regard to jurisdictional claims in published maps and institutional affiliations.



Copyright: © 2022 by the authors. Licensee MDPI, Basel, Switzerland. This article is an open access article distributed under the terms and conditions of the Creative Commons Attribution (CC BY) license (<https://creativecommons.org/licenses/by/4.0/>).

1. Introduction

Qinghai Province is the headwater region of the Yellow River, Yangtze River, and Lancang River. It is located in the northeast of the Tibetan Plateau (China), which is a region with high elevation and a fragile ecological environment. Land degradation and desertification have become serious environmental problems in this region, and the difficulty in recovering degraded land can result in serious soil erosion. According to the China Soil and Water Conservation Bulletin in 2019, the area of soil loss on the Tibetan Plateau was 61.0×10^4 km², which accounted for 23.1% of the entire land area of China. The area of soil loss in Qinghai Province was 16.2×10^4 km², of which 17.9% (12.5×10^4 km²) and 5.4% (3.7×10^4 km²) were attributable to wind erosivity and hydraulic erosivity, respectively. Therefore, a proper evaluation of wind–rainfall erosivity to soil-loss rates

represents a key step for zoning the most serious areas and identifying effective measures to prevent soil loss.

The response of the ecological environment of the Tibetan Plateau (TP) to the effects of climate change are highly sensitive and prominent [1]. Differences in topography, climate, and vegetation throughout Qinghai Province are notable, and almost all types of soil erosion can be found on TP [2,3]. Ecological degradation caused by compound soil erosion, which has become an environmental problem globally, is associated with obvious fluctuation, variability, and vulnerability of the ecological environment [4,5]. Moreover, wind/rainfall-induced erosion is more likely to occur in arid and semiarid regions [6–8]. The area of compound wind/rainfall erosion accounts for approximately 18.0% of the global area. Wind-induced erosion can occur in all four seasons, directly affecting the transmission and transformation of erosive substances, while rainfall-related erosion occurs mainly in the rainy season. Overlap of the two can prolong the period of soil erosion, and the superposition of wind- and rainfall-derived erosive processes has a mutually reinforcing effect that can result in a composite soil-erosion rate that is substantially more serious than that in an area exposed primarily to either wind erosion or rainfall erosion [9–12]. Thus, the compound effect of wind/rainfall erosivity is one of the root causes of the fragile environment of the Tibetan Plateau, but it is also an important manifestation of the fragile environment. Soil erosion is a major threat to soil health and soil–river ecosystem services in many regions globally [13,14]. There is evidence that the rate of soil erosion has increased under the effects of human activities such as deforestation, intensive agriculture, urbanization, and climate change [15]. Wind, rainfall, and freezing/thawing processes are the main climatic driving factors of soil erosivity. Moreover, in addition to the transformation of, and the disturbance to, the environment associated with human activities, variations in the spatiotemporal patterns of rainfall, rainfall intensity, and wind speed attributable to climate change are affecting the characteristics of soil erosion [16]. Therefore, research on wind/rainfall erosion climatic erosivity is required to provide references for soil conservation practices in Qinghai Province.

It has become an indisputable fact that the global climate is changing remarkably, with extreme weather events growing stronger and more frequent and lasting longer [17]. The TP is the largest and highest geographical unit in the world; it is of extreme importance to regional economic development and ecological security, as well as water resources and ecosystem functioning. Remarkably drastic environment changes have been observed in Qinghai during 2000–2020 [18], such as short periods of intense rainfall, strong winds, sand storms and high temperatures, which may have led to an increasing trend in the wind and rainfall erosivity in Qinghai. These changes have become the key factors increasing the soil-erosion risk. Some studies have analyzed the variation in wind or rainfall erosivity in Qinghai or Yellow river region, indicating an increasing trend of rainfall erosivity and a declining trend of wind erosivity. These studies provided useful information on the variation in wind or rainfall erosivity, but a further analysis is necessary for Qinghai as a whole.

The trend of wind/rainfall erosivity can provide information regarding the potential impact of wind/rainfall changes on soil erosion. It is particularly useful for Qinghai province, which is more sensitive to climate change and wind/water erosion because of its fragile biophysical conditions. In addition, a long series of observational data are restricted in Qinghai and most studies have not considered changes in meteorological station instrumentation and station relocation; moreover, the cause of annual changes in wind/rainfall erosion climatic erosivity are not clear at present. The most serious region of wind/rainfall erosivity has not been divided. Thus, whether the spatial-temporal qualities of wind/rainfall erosivity have become increasingly abnormal and what the impacts these altered patterns will have on soil erosion is worthy of discussion.

The characterization and proper evaluation of rainfall erosivity is commonly recognized as a challenging issue. Rainfall erosivity (R_{day} -factor) is the main dynamic factor causing soil water erosion, and it is also one of the main parameters used in modeling

soil erosion, sediment yield, and the hydrological environment [19,20]. The Revised Universal Soil Loss Equation model is commonly used globally in the evaluation of soil loss attributable to water erosion [21,22]. The method of a simple algorithm for half-monthly erosion is widely used in China, but this method will overestimate rainfall erosivity in regions with high erosion because its empirical formulas are based on data collected before 1984 from 71 precipitation stations across China, which means it must be calibrated prior to use [23]. However, the poor availability of long and complete time series of high-resolution rainfall data (minute rainfall) makes this approach quite difficult to apply, requiring the adoption of alternative simplified models relying on rainfall data with a daily, monthly, or annual scale. The model of the R-factor [24] is simple and can provide high estimation accuracy using daily rainfall with 2678 meteorological stations from 1980 to 2009 [25,26]; the mean relative error of the R-factor is 9.6%, and this has been adopted by many studies to analyze the rainfall erosivity in China or Qinghai. Thus, this method has wide applicability in Qinghai. Generally, the model of the R_{day} -factor plays an important role in generating quantitative estimates of rainfall erosivity and provides a scientific basis for how soil erosion could be prevented.

Wind-erosion climatic erosivity (C-factor) is an index used to evaluate wind-induced erosion. Three main methods are applied to the determination of wind-erosion climatic erosivity: the Chepil formula, the FAO formula, and the Skidmore formula, among which the FAO formula is the model used most widely [27]. These models require multiple inputs, such as soil, vegetation type, and climate data. Therefore, due to the data limitations, these models are generally unsuitable analyses of wind erosion at a large scale. In contrast, the wind-erosion climatic factor, commonly referred to as the indicator of wind erosion, can be used to measure the trend of climate change and its influence on wind-erosion conditions. Therefore, the spatial and temporal distribution difference of the C-factor often indicates the wind-erosion potential of the region.

Many studies have been undertaken on the spatial distribution of wind or rainfall erosivity in China, but the regional division of wind and rainfall climatic erosivity in Qinghai has not been reported. Moreover, the meteorological data used in such studies are mostly obtained from meteorological observing stations, and the heterogeneity of the data caused by changes in instrumentation and station relocation, which could affect the research results, is generally not considered. Thus, the determination of the variation in the spatiotemporal characteristics of wind/rainfall erosion climatic erosivity is highly important for the accurate evaluation of soil loss, protection of the environment, and interpretation of the effects of climate change in Qinghai Province.

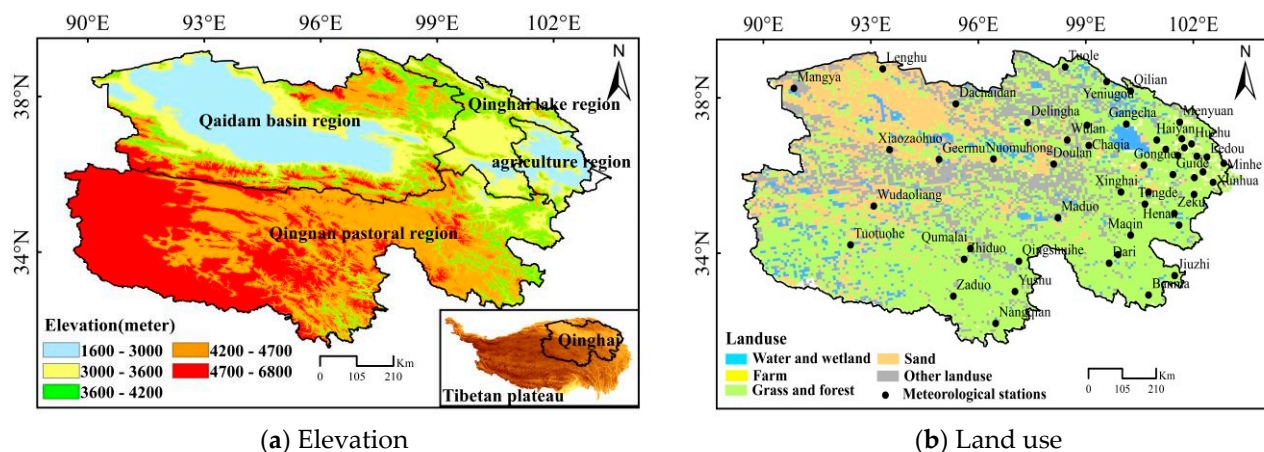
Climate variability affects the intensity of wind and rainfall erosion and that is the dominant factor controlling the desertification of the arid region. Affected by climatic warming, the R_{day} -factor shows an obvious increase trend in Tibetan plateau, which increases the risk of soil erosion [28], while the wind erosivity shows an declining trend in China because of decreases in wind speed [29–31]. Previous studies have focused on researching a single form of climatic erosivity in China, while the spatial and temporal aspects of how wind/rainfall erosivity varies in Qinghai have not been adequately studied, and the regional division of wind/rainfall erosivity due to the effects of global warming is not clear at present. The causes for the changing wind/rainfall erosivity in different regions should be discovered.

The main objectives of this study were as follows: (1) To analyze the spatiotemporal variations of wind/rainfall erosion climatic erosivity during 1970–2020 in Qinghai Province; (2) To divide the region based on wind/rainfall erosion climatic erosivity and analyze the differences for regional management purposes; (3) To determine the cause of annual change in wind/rainfall erosion climatic erosivity; (4) To examine the relationship between changes in wind/rainfall erosion climatic erosivity and soil erosion. The findings of this study will increase our understanding of wind/rainfall-erosion climatic erosivity in Qinghai Province, and provide a robust scientific reference for future soil- and water-conservation planning.

2. Data and Methods

2.1. Study Area

The topography of Qinghai Province is generally high in the west, north, and south and low in eastern and central areas (Figure 1a). The geomorphology is complex and diverse and includes the Tibet Plateau, the inland arid basin, and the Loess Plateau. The agricultural region, Qinghai Lake region, Qaidam Basin, and Qingnan pastoral region can be distinguished according to natural ecological characteristics. The area of sandy and bare land is $25.9 \times 10^4 \text{ km}^2$, accounting for 40% of the total land area of Qinghai Province (Figure 1b). Qinghai Province has a plateau continental climate. It has a short summer and long winter; high wind-speed values mainly occur in late winter and spring (November to April), while extreme rainfall mainly occurs in summer. The mean accumulative numbers was 486 times if the daily rainfall is not smaller 10 mm from 1970–2020, which had an obvious trend of increase with a rate of 27.0 times/10a ($p < 0.01$). The mean accumulative number was 300 times, if the daily wind speed is not smaller than 5 m/s during 1970–2020, with an obvious decreasing trend at a rate of 125.2 times/10a ($p < 0.01$).



(a) Elevation

(b) Land use

Figure 1. Distributions of (a) elevation and (b) land use and meteorological stations in Qinghai Province.

2.2. Data

Considering the homogeneity of data and unity of observation instruments, this study analyzed daily precipitation, mean temperature, maximum temperature, minimum temperature, wind speed, pressure, humidity, and sunshine hours recorded at 50 meteorological stations in Qinghai Province 1970–2020, which were provided by the Qinghai Climate Center. The longest time series is 51 years, and 49 meteorological stations provided data covering more than 40 years. All data underwent thorough quality control.

2.3. Method

2.3.1. Wind-Erosion Climatic Erosivity

Wind-erosion climatic erosivity is a measure of the potential climatic impact of wind erosion, which is an indicator of land desertification and expressed as the wind-erosion climatic factor index. The influence of climatic conditions on wind erosion is not only limited to wind effects but also is the result of the combined effect of wind speed, precipitation, temperature, and other factors [32,33]. Chepil (1962) proposed that climatic factors determine the level of wind erosion, and thus the wind-erosion climatic factor index was proposed and incorporated in the calculation of the wind-erosion equation [34].

Subsequently, the United Nations Food and Agriculture Organization (FAO) revised the Chepil formula to the following (FAO, 1979) [35]:

$$C = \frac{1}{100} \sum_1^{12} \left\{ u_i^3 [(ETP_i - p_i) / ETP_i] d_i \right\} \quad (1)$$

where C is the monthly wind-erosion climatic erosivity (dimensionless), and u_i , ETP_i , p_i , and d_i are the mean monthly wind speed at 2 m height (m/s), monthly potential evapotranspiration (mm), monthly precipitation (mm), and number of days (d) in a month, respectively.

The monthly evapotranspiration is calculated as follows:

$$ET_0 = \frac{0.408\Delta(R_n - G) + \gamma \frac{900}{T+273} U_2(e_s - e_a)}{\Delta + \gamma(1 + 0.342U_2)} \quad (2)$$

where ET_0 is potential evapotranspiration (mm/d), R_n is surface net radiation ($\text{MJ}/(\text{m}^2 \cdot \text{d})$), T is the mean temperature ($^\circ\text{C}$), U_2 is wind speed (m/s) at 2 m height, e_s and e_a are saturated vapor pressure (KP_a) and actual vapor pressure (KP_a), respectively, Δ is the slope of saturated vapor pressure ($\text{KP}_a/^\circ\text{C}$), and γ is the psychometric constant ($\text{KP}_a/^\circ\text{C}$).

2.3.2. Rainfall Erosivity

The commonly used rainfall erosivity method is based on rainfall at hourly, daily, monthly, and annual scales. In comparison with annual and monthly scales, the accuracy of rainfall-erosivity estimation based on daily rainfall is more reliable, and such data are easily obtained and widely used. In this study, the method of R_{day} -factor was used to estimate rainfall erosivity during April–November [36]; that is, the period of solid precipitation from December to the following March was ignored. The daily R_{day} -factor is calculated using the following equation:

$$R_{\text{day}} = a P_d^{1.7265}, \quad (3)$$

where P_d is daily erosive rainfall (rainfall: ≥ 10 mm), and a is 0.3937 during the warm season (May–September) and 0.3101 during the cold season (October to the following April). The monthly and annual R_{day} -factor can be obtained by cumulative summation of the daily erosivity.

2.3.3. K-Means Clustering Method

The K-means clustering method is a typical unsupervised clustering algorithm, which is mainly used to automatically classify similar samples into a class. The core principle is to first determine the constant K , which represents the final number of clustered categories. The K sample points are then randomly selected as centroids, and the similarity between each sample and the K centroids is calculated. Each sample is classified into the class belonging to the centroid with which it has greatest similarity [37,38]:

$$dist(x, c) = \sqrt{\sum_{t=1}^m (x_t - c_t)^2} \quad (4)$$

where $dist(x, c)$ is the Euclidean distance of sample x to centroid c , and x_t and c_t represent the principal component t of x and c , respectively. When a centroid no longer changes or has reached the specified number of convergences, the centroids of each sample and each class are finally determined. In this study, wind/rainfall erosion climatic erosivity data for Qinghai Province were standardized, and then wind/rainfall-erosion climatic erosivity was divided into three types via K-means clustering analysis.

2.3.4. Other Methods

This study used simple linear regression, the Mann–Kendall (M–K) test, and continuous wavelet transform to explore the temporal variation in the wind/rainfall erosivity series [39]. The M–K analysis, as proposed separately by Mann (1945) and Kendall (1990),

is widely used for the trend analysis of time series. The advantage of the M–K test is that a series does not need to conform to a certain sampling distribution, thereby avoiding the potential influence of outliers. In this study, the M–K test was used to detect trends and abrupt changes. The continuous wavelet transform method, introduced by Torrence and Compo (1998), is widely used to detect periodicity in a time series. Among many wavelet functions, the Morlet wavelet function provides an acceptable balance between time and frequency localization, and thus is considered most suitable for studying the temporal variation in wind/rainfall erosivity.

3. Results

3.1. Characteristics of Wind/Rainfall Erosion Climatic Erosivity

3.1.1. Spatial Distribution of Wind/Rainfall-Erosion Climatic Erosivity

Figure 2a shows the spatial distribution of the annual wind-erosion climatic erosivity of the studied 51 years (1970–2020), as calculated using the FAO model. Generally, the range of the value of the C-factor across Qinghai Province was relatively large, ranging from 130 in the northwest to 2.3 in the southeast. Areas with a high value of the annual C-factor (50–130) are evident in the western Qaidam Basin, the Qinghai Lake region, and the western Qingnan pastoral region. The C-factor was in the range 24–44 in the central-eastern Qaidam Basin and the center of the Qingnan pastoral region, while relatively low values (2.3–23) occurred in the agricultural region and the southeast of the Qingnan pastoral region. The spatial distribution of the C-factor in Qinghai Province is consistent with topography and land-use change.

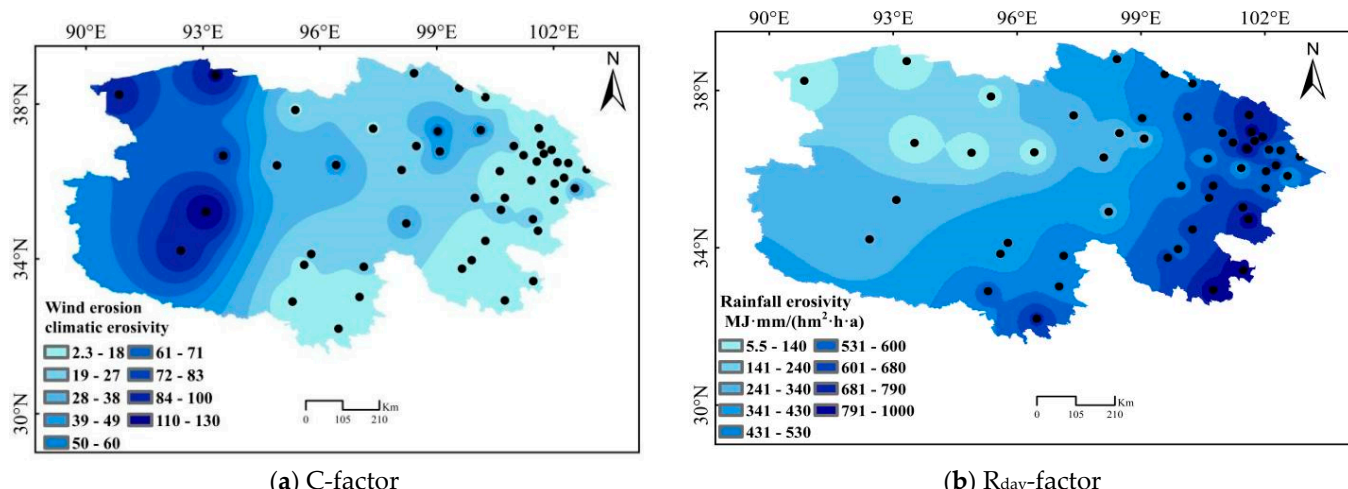
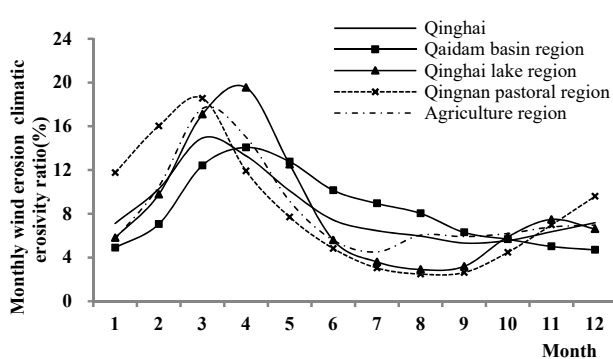


Figure 2. Spatial distributions of (a) annual wind-erosion climatic erosivity (C-factor) and (b) rainfall erosivity (R_{day} -factor) in Qinghai Province averaged over 1970–2020.

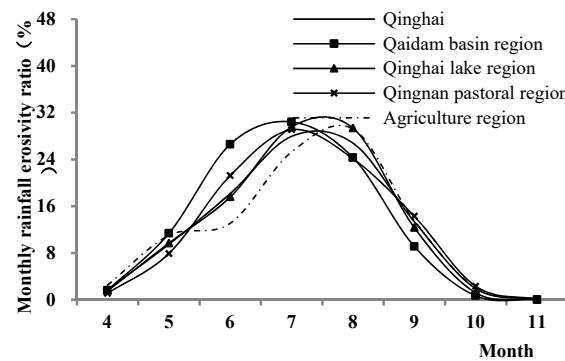
Figure 2b shows the spatial distribution of the annual rainfall erosivity, with values in the range of 5.3–1048.2 MJ·mm/(hm²·h·a). Areas with annual rainfall erosivity of <300.0 MJ·mm/(hm²·h·a) are evident only in the Qaidam Basin, with the lowest value recorded in Xiao Zaohuo. Areas with annual rainfall erosivity of >700 MJ·mm/(hm²·h·a) are primarily found in the southeast of the Qingnan pastoral region and the agricultural region, especially in Jiuzhi, Huangzhong, and Datong. Overall, high values of the C-factor occurred in the Qaidam Basin, the western Qingnan pastoral region, and the Qinghai Lake region, while high values of the R_{day} -factor occurred in the Qingnan pastoral region and the agricultural region. The zone of combined wind/rainfall-erosion climatic erosivity aggravated soil erosion more than in areas exposed primarily to wind erosion or rainfall erosion.

3.1.2. Mean Monthly Variations of Wind/Rainfall-Erosion Climatic Erosivity

The mean monthly C-factor in Qinghai province shows a single-peaked distribution, with a maximum ratio of 14.9% in March and the lowest ratio of 5.3% in September (Figure 3a). The period with relatively high ratios of the monthly C-factor in Qinghai Province was generally late winter and spring (February–May), accounting for a substantial proportion of 48.6%. Among the subregions, the ratio of the mean monthly C-factor in the Qinghai Lake region (58.6%) was substantially higher than that in other regions (46.3–4.2%) February–May.



(a) Monthly C-factor ratio



(b) Monthly R_{day} -factor ratio

Figure 3. Variations of ratio of monthly (a) wind-erosion climatic erosivity(C-factor) and (b) rainfall erosivity (R_{day} -factor) to annual values in Qinghai Province.

The ratio of the mean monthly R_{day} -factor also shows a single-peaked distribution, with a maximum ratio of 28.0% in July and the lowest ratio of 0.1% in November. The period with the highest R_{day} -factor values in Qinghai Province was summer, accounting for a substantial proportion of 72.9% (Figure 3b). The ratio of the mean monthly R_{day} -factor in the four subregions (67.6–81.3%) in summer was substantially higher than that in other seasons.

Overall, high values of the C-factor occurred in late winter and spring, while high values of the R_{day} -factor occurred in summer. Wind-erosion climatic erosivity and rainfall erosivity were obviously asynchronous on an annual basis, and the period of their combination extended the time of soil erosion.

3.2. Trend Variation in Wind/rainfall Erosion Climatic Erosivity

3.2.1. Annual Trend Variation in Wind/Rainfall Erosion Climatic Erosivity

The mean annual C-factor was 25.8 during 1970–2020 (Figure 4a), which had an obvious trend of decrease with a rate of 6.5/10a ($p < 0.01$). There was a high value in the 1970s and it began to decrease obviously after the 1980s. The mean annual C-factor was 9.8, 18.0, 26.7, and 48.5 in the agricultural region, Qinghai Lake region, Qingnan pastoral region, and Qaidam Basin, respectively, and the mean annual C-factor in each of the subregions had a trend of decrease with a rate of 1.6, 2.9, 6.6, and 15.1 /10a, respectively ($p < 0.01$). In particular, there was significant decreasing trend in both the Qaidam Basin and the Qingnan pastoral region. Under the background of climate change, the climate of Qinghai Province has exhibited increases in temperature and humidity since the 2000s, and the government had undertaken certain ecological protection projects, which have caused a marked decrease in the actual observed wind speed, which is reflected in the significant decrease in the C-factor.

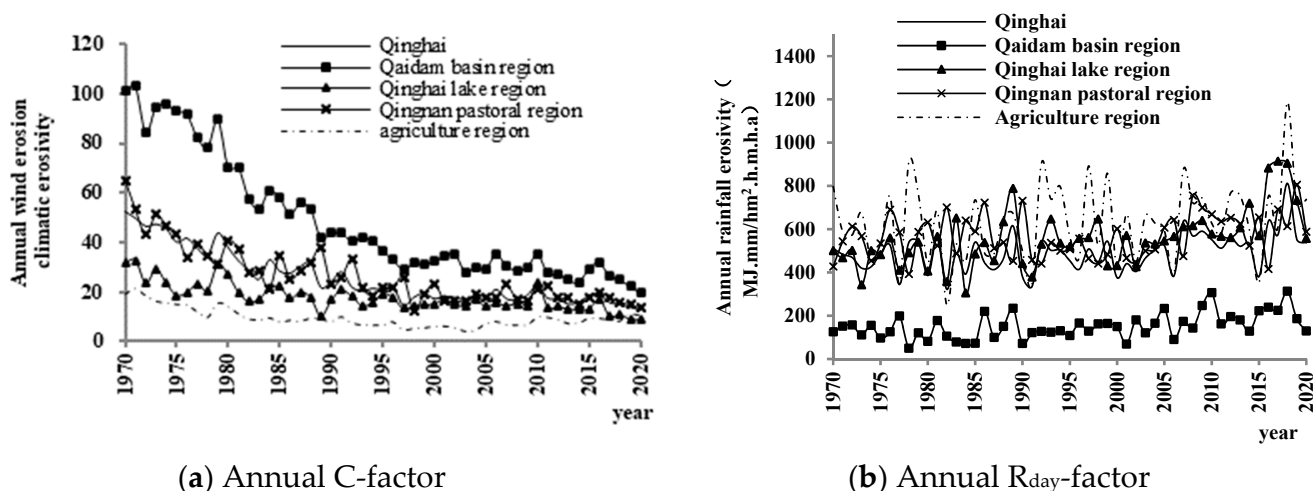


Figure 4. Annual variations of (a) wind-erosion climatic erosivity (C-factor) and (b) rainfall erosivity (R_{day} -factor) in Qinghai Province during 1970–2020.

The mean annual R_{day} -factor in Qinghai Province 1970–2020 was $491.6 \text{ MJ} \cdot \text{mm}/(\text{hm}^2 \cdot \text{h} \cdot \text{a})$ with a rate of increase of $24.0 \text{ MJ} \cdot \text{mm}/(\text{hm}^2 \cdot \text{h} \cdot \text{a})/10\text{a}$ ($p < 0.02$) (Figure 4b). The mean annual R_{day} -factor in the two periods of 1970–1999 and 2000–2020 was 467.0 and 526.8 $\text{MJ} \cdot \text{mm}/(\text{hm}^2 \cdot \text{h} \cdot \text{a})$, respectively, with an obvious trend of increase in both periods. Over the past 51 years, the mean annual R_{day} -factor in the agricultural region, Qingnan pastoral region, Qinghai Lake region, and Qaidam Basin was 628.4, 565.7, 558.2, and $152.7 \text{ MJ} \cdot \text{mm}/(\text{hm}^2 \cdot \text{h} \cdot \text{a})$, respectively, with a rate of increase of 32.2, 13.9, 52.2, and $20.0 \text{ MJ} \cdot \text{mm}/(\text{hm}^2 \cdot \text{h} \cdot \text{a})/10\text{a}$ ($p < 0.02$), respectively, but the only obvious trend of increase was in the Qinghai Lake region and the agricultural region.

In conclusion, the changes in wind-erosion climatic erosivity and rainfall erosivity in Qinghai Province exhibit obvious differences over the recent 51 years; the C-factor has decreased obviously, while the R_{day} -factor has increased significantly. According to recent research, the disparity in the trend of change in temperature between the Tibet Plateau and its surrounding regions is the main reason for the decrease in wind speed on the plateau since the beginning of the 21st century [40,41]. Coupled with the strong heating of the plateau in spring, the time of onset of the plateau's summer monsoon has advanced and the intensity has strengthened, which can increase the proportion of annual precipitation in spring and summer [42].

3.2.2. Spatial Change Rates Distribution of Wind/Rainfall Erosion Climatic Erosivity

The annual trend rate of the C-factor showed a significant decrease for most stations in Qinghai Province, and the rate of decrease was greater in the west than in the east (Figure 5a). The trend of decrease in the Qaidam Basin and the western Qingnan pastoral region was more obvious. Overall, 43 meteorological stations (approximately 86%) showed a significant trend of decrease with a rate of $0.3\text{--}55.2/10\text{a}$ ($p < 0.01$), six stations showed a trend of decrease that failed the significance test ($p < 0.01$), and only Yushu showed an obvious trend of increase with a rate of $0.3/10\text{a}$ ($p < 0.01$).

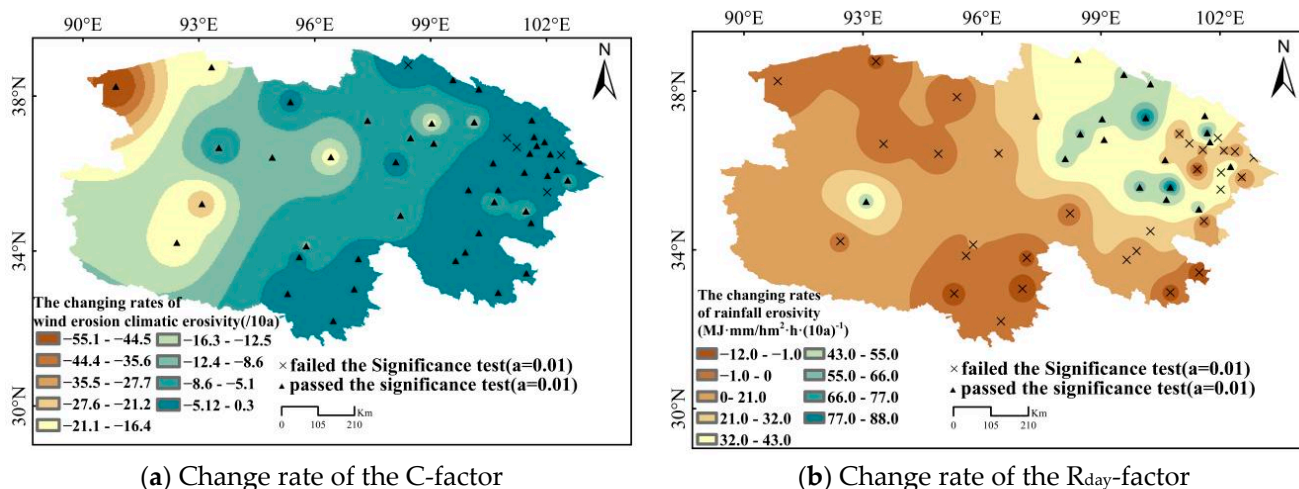


Figure 5. Spatial distributions of change rates of (a) wind-erosion climatic erosivity (C-factor) and (b) rainfall erosivity (R_{day} -factor) in Qinghai Province during 1970–2020.

The annual trend of the R_{day} -factor showed a trend of increase in most regions except at eight stations in the northwest and southeast of Qinghai Province (Figure 5b). Overall, 41 stations (approximately 82%) showed a trend of increase with a rate of 2.0–88.9 MJ·mm/(hm²·h·a)/(10a), but only 19 stations passed the significance test ($p < 0.01$). In particular, the trend of increase in both the agricultural region and the Qinghai Lake region was obvious. Eight stations (Guide, Dachaidan, Lenghu, Henan, Jiuzhi, Qingshuihe, Zaduo, and Banma) showed a trend of decrease with a rate of 0.6–12.5 MJ·mm/(hm²·h·a)/10a, but all stations failed the significance test ($p < 0.01$). Overall, the trend of variation in the C-factor showed significant decrease in most regions. Although the trend of variation in the R_{day} -factor showed increase in most regions, only 38% of the region showed an obvious increase that passed the significance test.

3.3. Abrupt Change Point Analysis and Periodic Oscillation Analysis

3.3.1. M-K Analysis for Wind/Rainfall Erosion Climatic Erosivity

The M-K test was used to detect trends and abrupt change points in wind/rainfall erosion climatic erosivity in Qinghai Province and its subregions. According to the UF line illustrated in Figure 6, the wind-erosion climatic erosivity in Qinghai Province and the four subregions showed a downward trend during 1970–2020 with no abrupt change points. Conversely, rainfall erosivity showed an upward trend between 1973 and 1979 and a downward trend between 1980 and 2006, with a significant change point in 2007 ($p < 0.05$) that was followed by an upward trend from 2008 to 2020, which was significant after 2010. The Qaidam Basin region had a change point in 2004 and in 2006. The change point in both the Qinghai Lake region and the Qingnan pastoral region occurred in 2007. All subregions had a significant upward trend after 2008. Details on the subregions are illustrated in Figure 6c–j.

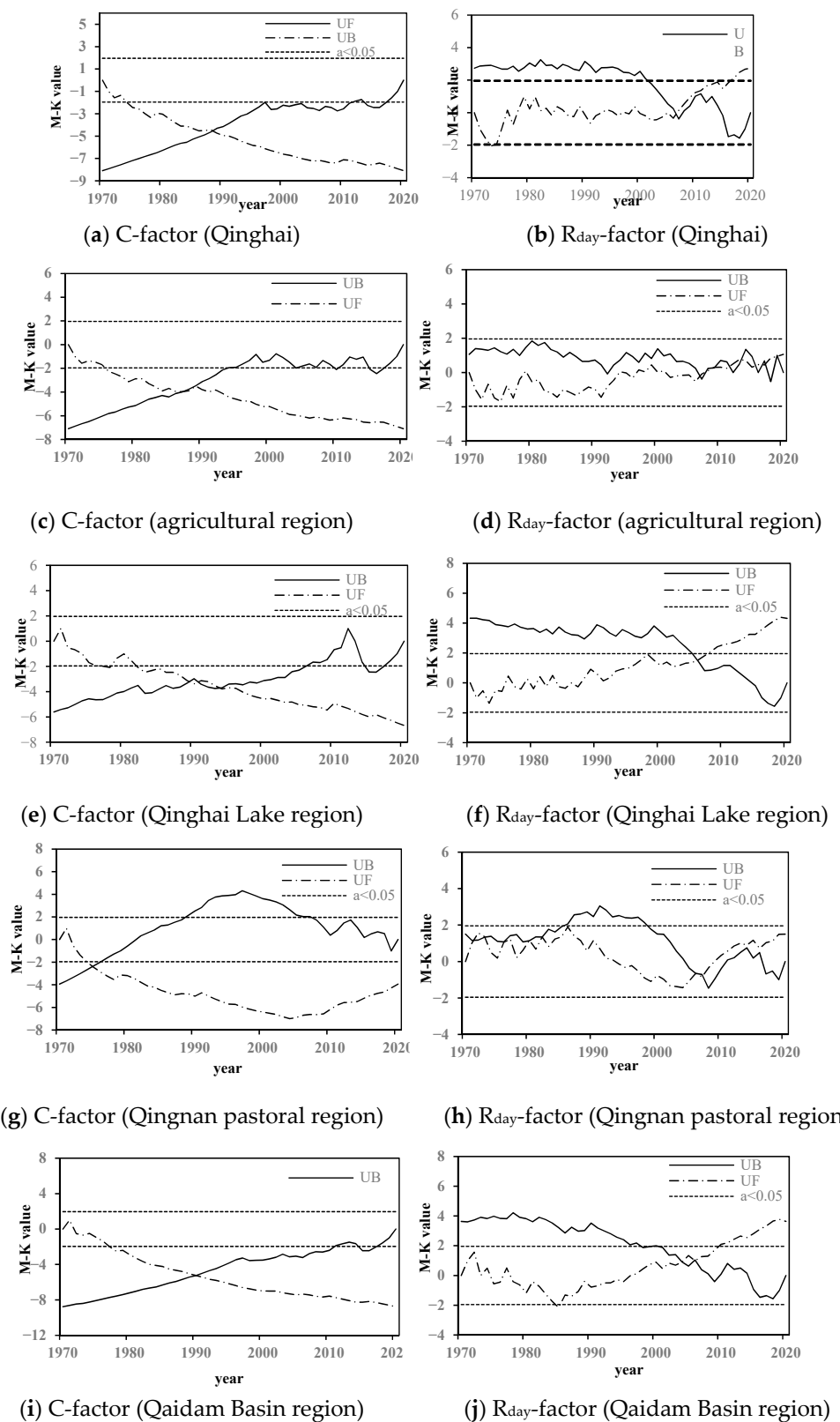


Figure 6. M–K test results for the annual wind-erosion climatic erosivity (C-factor) and rainfall erosivity (R_{day} -factor) in Qinghai Province and its subregions. UF and UB represent the statistics of the forward and backward sequence, respectively.

3.3.2. Periodic Oscillation Analysis of the Annual Wind/rainfall Erosion Climatic Erosivity

The continuous wavelet transform was used to analyze the periodic variation in the annual wind/rainfall erosion climatic erosivity in Qinghai province during 1970–2020 (Figure 7). A period of 8.5 years in wind-erosion climatic erosivity was detected, which was significant above the 95% confidence level (Figure 7a). Periods of 2.0, 5.0, and 8.0 years in rainfall erosivity were detected, and the interannual oscillations at the 2.0- to 8.0-year scale were significant at the 95% confidence level (Figure 7b).

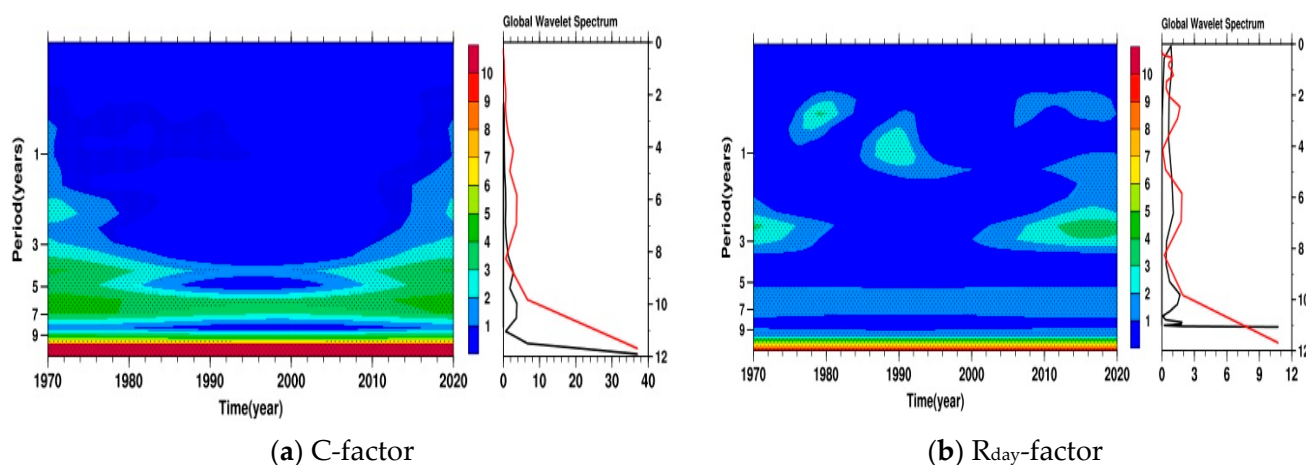


Figure 7. Period analysis of (a) wind-erosion climatic erosivity (C-factor) and (b) rainfall erosivity (R_{day} -factor) in Qinghai Province during 1970–2020.

3.4. Group Division of Wind/Rainfall Erosion Climatic Erosivity

Wind and rainfall are the principal climatic factors that affect soil erosion, and the area of most serious erosion on the Loess Plateau is a region in which the areas of wind-erosion climatic erosivity and rainfall erosivity overlap with annual rainfall of approximately 400 mm. Therefore, according to the influence of the two factors on soil erosion, the K-means clustering method was used to divide the wind/rainfall erosion climatic erosivity in Qinghai Province; the number of clusters k increased from 2 to 7. It can be seen that the curve has an obvious inflection at $k = 3$ point (Figure 8), thus, this paper divides the wind/rainfall erosion climatic erosivity into three types according to the elbow (Figure 9). The first represents regions dominated by wind climatic erosivity, which include Lenghu, Mangya, Xiaozahuo, Wudaoliang, and Tuotuohe (Table 1), where surface vegetation is sparse and most areas are desert or saline land. The second represents regions dominated by rainfall erosivity with higher precipitation and greater coverage of surface vegetation. The third represents regions with high elevation and a fragile ecological environment; the surface vegetation of this type is better than that of the first type and poorer than that of the second type. The most serious land erosion occurs in the third type, which accounts for 34.3% of the entire land area of Qinghai Province, has annual rainfall of 300–400 mm, and elevation of 2500–4400 m. The distribution of wind/rainfall erosion climatic erosivity is broadly consistent with the distributions of rainfall and elevation. The rate of soil erosion in areas affected by the combined effects of wind-erosion climatic erosivity and rainfall erosivity is significantly higher than that in areas affected primarily either by wind-erosion climatic erosivity or by rainfall erosivity. Therefore, attention should focus on regions affected by combined wind/rainfall erosion climatic erosivity to prevent soil erosion.

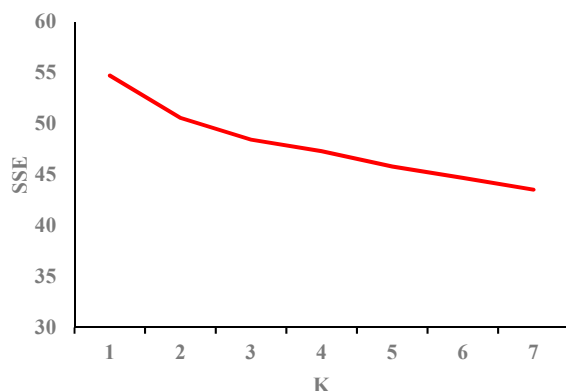


Figure 8. The cluster number K of k-mean.

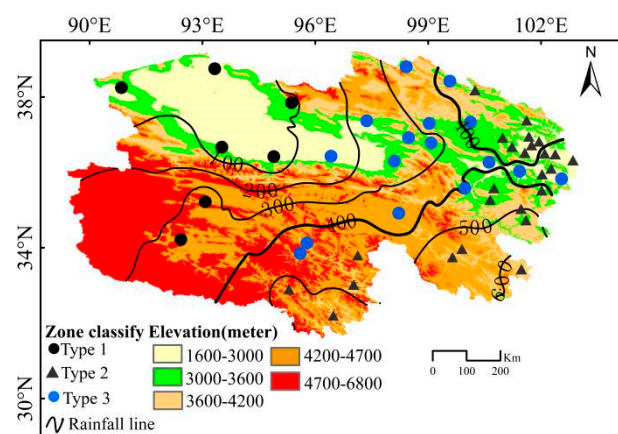


Figure 9. Zone division of wind/rainfall erosion climatic erosivity in Qinghai Province.

Table 1. Three types of wind/rainfall erosion climatic erosivity in Qinghai Province with k-means clustering method.

Classify	Stations
Type 1	Lenghu, Mangya, Xiaozaoahuo, Wudaoliang, Tuotuohe
Type 2	Xining, Ledou, Minhe, Huangyuan, Datong, Huangzhong, Hualong, Huzhu, Tongren, Pingan, Jianzha, Menyuan, Qilian, Guinan, Zeku, Maqin, Dari, Jiuzhi, Yushu, Nangqian, Qingshuihe, Zaduo, Banma, Henan, Gande, Tongde
Type 3	Yeniugou, Gangcha, Tianjun, Xinghai, Xunhua, Guide, Tuole, Gonghe, Delingha, Wulan, Doulan, Chaqia, Qumalai, Zhiduo, Maduo, Nuomuhong, Haiyan, Geermu, Dachaidan

4. Discussion

4.1. Temporal Variation in Three Types of Climatic Erosivity

To illustrate the comprehensive variation characteristics of wind/rainfall erosion climatic erosivity in Qinghai Province, the change in climatic erosivity in the study area was further examined according to the three regional types distinguished by wind/rainfall erosion climatic erosivity. The mean annual C-factor in type 1 regions was 99.5, with a rate of decrease of 24.8/10a ($p < 0.01$) (Figure 10). The R_{day} -factor was 111.2 MJ·mm/(hm²·h·a) and the rate of increase was 10.9 MJ·mm/(hm²·h·a)/10a ($p < 0.01$). The C-factor of type 2 regions was 9.1 with a rate of decrease of 2.0/10a ($p < 0.01$), and the R_{day} -factor was 675.0 MJ·mm/(hm²·h·a) with a rate of increase of 31.2 MJ·mm/(hm²·h·a)/10a ($p < 0.01$). The C-factor of type 3 regions was 27.9 and the rate of decrease was 7.3/10a ($p < 0.01$), and the R_{day} -factor was 300.5 MJ·mm/(hm²·h·a) with a rate of increase of 20.1 MJ·mm/(hm²·h·a)/10a ($p < 0.01$). The area of type 3 regions was 32.2×10^4 km², accounting for 34.3% of the

entire study area, mainly distributed in the eastern Qaidam Basin, the Qinghai Lake region, and the upper reaches of the Yellow River. Affected by climate change, wind-erosion climatic erosivity in Qinghai Province showed a trend of decrease, while rainfall erosivity showed a trend of increase. The wind/rainfall composite erosivity area accounted for a large proportion of the land area in Qinghai Province, and the ecological environment of this region was obviously fragile coupled with its dense population distribution. Therefore, measures should be taken to prevent change in soil erosion caused by wind/rainfall-erosion climatic erosivity.

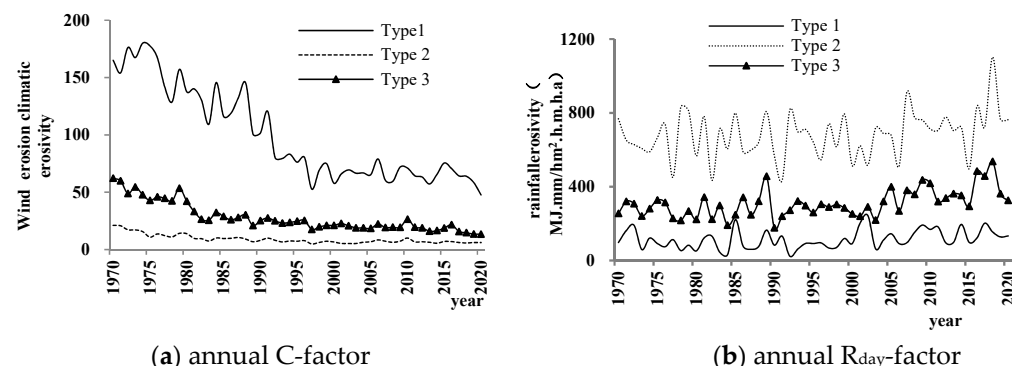


Figure 10. Three types of variation in (a) wind-erosion climatic erosivity (C-factor) and (b) rainfall erosivity (R_{day} -factor) in Qinghai Province during 1970–2020.

The amount of rainfall and number of rainy days in Qinghai Province have increased markedly since the 2000s [43], providing positive enhancement of the climatic conditions suitable for vegetation restoration. Additionally, continuous implementation of ecological protection projects in Qinghai Province has been extremely beneficial to restoration of the ecological environment since 2000. Thus, the normalized difference vegetation index in Qinghai Province has shown a trend of increase from 2003 to 2017 [44,45]. According to the Qinghai Bulletin Report of Soil and Water Conservation in 1995 and 2020 [46,47], the land area experiencing wind and hydraulic erosion in Qinghai Province was 12.9×10^4 and $5.3 \times 10^4 \text{ km}^2$, respectively, in 2015, and 12.5×10^4 and $3.7 \times 10^4 \text{ km}^2$, respectively, in 2019; that is, both showed a trend of decrease and the area experienced a significant decrease in hydraulic erosion. The C-factor in Qinghai Province showed a trend of decrease, which should be reflected in a reduction in the range and intensity of wind erosion, whereas the increase in the amount of rainfall should lead to increased rainfall erosivity and expansion of the area experiencing water erosion. However, the results show the opposite situation, apparently contradicting the trends of wind and hydraulic erosion areas based on soil-and water-conservation monitoring data. One possible explanation is that the increased vegetation coverage attributable to the increased rainfall and higher number of rainy days prevents worsening water erosion. Therefore, the increase in vegetation coverage inhibited the wind/rainfall erosivity in Qinghai Province to a certain extent.

4.2. Cause Analysis

The partial correlation coefficient and significance tests between the wind/rainfall erosion climatic erosivity and meteorological elements were calculated to show their relations (Table 2). The C-factor had positive correlation with wind speed, annual cumulative numbers of wind speed (wind speed not smaller than 5 m/s), and sunshine duration in all subregions, and significant negative correlation with annual precipitation and temperature in all subregions. Additionally, the trend of annual wind speed in three regions showed an obvious decrease, with a rate of 0.1–0.3 m/s/10a ($p < 0.05$) (Table 3). Qinghai showed a significant decrease trend in annual cumulatives wind-speed times with a rate of 14.7–56.2 time/10a ($p < 0.05$), and the trends of annual temperature and annual rainfall both showed obvious increases and passed the significance test level ($p < 0.05$). Thus, wind

speed, temperature, rainfall, and sun duration are the principal factors known to impact the variation in wind-erosion climatic erosivity.

Table 2. Partial correlation coefficients and significance test of annual wind/rainfall-erosion climatic erosivity and meteorological elements.

Meteorological Elements	C-Factor			R_{day} -Factor		
	Type 1	Type 2	Type 3	Type 1	Type 2	Type 3
Annual temperature	−0.492 *	−0.484 *	−0.523 *	0.296 *	0.220	0.506 *
Annual rainfall	−0.382 *	−0.279 *	−0.440 *	/	/	/
Sunshine duration	0.256 *	0.335 *	0.367 *	−0.346 *	−0.385 *	−0.559 *
Wind speed	0.979 *	0.881 *	0.844 *	−0.232	−0.011	−0.419 *
Humidity	−0.167	0.026	−0.193	0.134	−0.039	0.160
Evapotranspiration	0.468 *	0.157	0.237 *	−0.065	−0.099	−0.240 *
Annual cumulative numbers of wind speed (wind speed not smaller than 5 m/s)	0.989 *	0.963 *	0.985 *	/	/	/
Rainfall intensity	/	/	/	0.509 *	0.232	0.322 *
Annual erosive rainfall	/	/	/	0.961 *	0.675 *	0.567 *
Rainy days (rainfall amount not smaller than 10 mm)	/	/	/	0.864 *	0.891 *	0.910 *
Annual cumulative times of rainfall (rainfall amount not smaller than 25 mm)	/	/	/	0.283 *	0.808 *	0.801 *

* denotes passing the 0.05 significance test level.

Table 3. Rate of change and significance of annual variations of meteorological elements 1970–2020.

Meteorological Elements	Subregions		
	Type 1	Type 2	Type 3
Changing rate in annual temperate ($^{\circ}\text{C}\cdot 10\text{a}^{-1}$)	0.52 *	0.45 *	0.41 *
Changing rate in annual rainfall ($\text{mm}\cdot 10\text{a}^{-1}$)	9.40 *	9.10 *	13.10 *
Changing rate in annual sunshine duration ($\text{h}\cdot 10\text{a}^{-1}$)	−45.3 *	−39.2 *	−42.9 *
Changing rate in annual wind speed ($\text{m/s}\cdot 10\text{a}^{-1}$)	−0.30 *	−0.10 *	−0.13 *
Changing rate in annual humidity ($\%\cdot 10\text{a}^{-1}$)	−0.02	−0.80 *	−0.10
Changing rate in annual cumulative numbers of wind speed (time $\cdot 10\text{a}^{-1}$)	−54.2 *	−14.7 *	−56.2 *
Changing rate in annual evapotranspiration ($\text{mm}\cdot 10\text{a}^{-1}$)	−86.70 *	−5.60	−10.30
Changing rate in annual rainfall intensity ($\text{mm}\cdot \text{d}\cdot 10\text{a}^{-1}$)	−0.31	−0.37	0.40
Changing rate in annual erosive rainfall ($\text{mm}\cdot 10\text{a}^{-1}$)	4.00 *	8.00 *	6.20 *
Changing rate in annual rainy days ($\geq 10 \text{ mm}$) ($\text{d}\cdot 10\text{a}^{-1}$)	0.30 *	0.50 *	0.60 *
Changing rate in annual cumulative times of rainfall (rainfall amount not smaller than 25 mm) (time $\cdot 10\text{a}^{-1}$)	−0.10	3.24 *	2.23 *

* denotes passing the 0.05 significance test level.

The rainfall erosivity value would be zero if the daily precipitation was $<10 \text{ mm}$; that is, the erosivity of high-intensity precipitation is much larger than that of low-intensity precipitation because of the increase in the frequency of high-intensity precipitation. Therefore, partial correlation coefficients of R_{day} -factor and erosive rainfall, rainfall days, rainfall intensity, and other meteorological elements were calculated to analyze the cause of change in the R_{day} -factor. The results showed that the change of R_{day} -factor in three subregions had obvious positive correlation with erosive rainfall, annual cumulative times of rainfall (rainfall amount not smaller than 25 mm), and the number of rainy days, and significant negative correlation with sunshine duration in three subregions. Meanwhile, the annual erosive rainfall amount and the number of rainfall days (rainfall $\geq 10 \text{ mm}$) both increased with a rate of 4.0–8.0 $\text{mm}/10\text{a}$ and 0.3–0.6 $\text{d}/10\text{a}$ ($p < 0.05$), respectively (Table 3), and annual cumulative times of rainfall (rainfall amount not smaller 25 mm) increased with a rate of 2.2–3.2 time/ 10a in type 2 and type 3 regions ($p < 0.05$). Sunshine duration showed a trend of decrease in three subregions with a rate of 39.2–45.3 $\text{h}/10\text{a}$ ($p < 0.05$). Thus,

the annual erosive rainfall amount, number of rainy days, and sunshine duration are the principal factors known to impact the variation in rainfall erosivity.

4.3. Influence of Wind/Rainfall Erosion Climatic Erosivity

Under the background of global warming since the beginning of the 21st century, wind-erosion climatic erosivity has decreased significantly and rainfall erosivity has increased significantly in Qinghai Province. On the one hand, the increase in precipitation in the study area has provided positive climatic conditions suitable for the restoration of the vegetation of the fragile ecological environment. The continuous implementation of ecological protection projects by China's government has significantly increased the vegetation coverage in Qinghai Province, which has effectively reduced soil erosion caused by wind and rainfall. On the other hand, extreme rainfall is more likely to cause debris flows, landslides, and other related disasters. The climatological risk of soil water erosion has increased in extent, and the increase in rainfall erosivity has increased the risk of soil loss. Therefore, the conservation projects in the regions where rainfall erosivity has increased significantly should be adjusted and strengthened. Moreover, the reduction in wind erosion is extremely beneficial for ecological restoration. However, it remains necessary to strengthen ecological protection projects in the regions at risk of combined wind/rainfall erosion by returning farmland to forest or grassland and by increasing vegetation cover, not only to control soil loss but also to intercept the transmission of sediment before it enters the rivers. Therefore, it would be worthwhile to further investigate the mechanisms of wind/rainfall erosion climatic erosivity to prevent soil erosion in the future. Furthermore, despite the importance of climatic variation in relation to soil erosion, the influence of socioeconomic and environmental factors cannot be neglect. This study considered only natural factors related to the trends of change in wind/rainfall erosion climatic erosivity, and the importance of human activities, land use, vegetation, and environmental elements in relation to soil loss was not discussed. These factors, which do play important roles in regional soil loss, should be considered in future development and implementation of soil conservation measures in Qinghai Province.

5. Conclusions

In this study, the spatiotemporal distributions and causes of wind/rainfall-erosion climatic erosivity in Qinghai Province were analyzed based on precipitation and wind speed data acquired at 50 meteorological stations in Qinghai Province 1970–2020. The C-factor in Qinghai Province decreased at a rate of 6.5/10a over the past 51 years, while rainfall erosivity increased at a rate of $24.0 \text{ MJ} \cdot \text{mm}/(\text{hm}^2 \cdot \text{h} \cdot \text{a})/10a$. The monthly wind-erosion climatic erosivity and rainfall erosivity both showed a single-peaked distribution. No breakpoint were detected for C-factor in Qinghai province, and there was a breakpoint in 2007 for R_{day}-factor in Qinghai province. Although wind-erosion climatic erosivity showed a declining trend and rainfall erosivity showed an increasing trend in recent 51 years in Qinghai Province, the soil-loss area attributed to wind erosivity was serious than hydraulic erosivity, so wind- and rainfall-induced soil erosion is the result of multiple factors. This study only investigated the influence of meteorological factors on wind-induced soil erosion, and further more comprehensive studies on soil erosion are needed.

Wind-erosion climatic erosivity occurred mostly in late winter and spring, while rainfall erosivity occurred mainly in summer. Wind-erosion climatic erosivity and rainfall erosivity were obviously asynchronous on an annual basis, and the period of their combination extended the time of soil erosion. It was meaningful to focus on measures adopted to prevent the negative influence of combined wind/rainfall erosivity on soil erosion. The wind/rainfall erosion climatic erosivity in Qinghai Province was divided into three types using the K-means clustering method. Type 3 regions, which experienced the greatest soil erosion, had annual rainfall of 300–400 mm and elevation of 2500–4400 m, and accounted for 34.3% of the total land area of Qinghai Province.

Wind speed, temperature, rainfall, and sunshine duration are key factors known to impact the variation in wind-erosion climatic erosivity, while annual erosive rainfall, number of rainy days, and sunshine duration are the main factors known to impact the variation in rainfall erosivity. So the ecological protection projects in the regions where rainfall erosivity has increased significantly should be adjusted and strengthened in order to prevent soil loss.

Author Contributions: Y.L. performed the data analysis and participated in the writing of the manuscript. G.G. and H.L. performed the conceptualization and methodology, L.L., Z.F. and T.W. helped cause analysis and participated in the discussion on results. All authors have read and agreed to the published version of the manuscript.

Funding: This research was supported by the Science and Technology Department Program of Qinghai in China (No. 2022-ZJ-767), and the National Nature Science Foundation of China (No. U20A2081).

Institutional Review Board Statement: Not applicable.

Informed Consent Statement: Not applicable.

Data Availability Statement: The authors confirm that the data supporting the findings of this study are available within the article.

Acknowledgments: We acknowledge support from the above funding projects.

Conflicts of Interest: The authors declare no conflict of interest.

References

1. Zhang, G.-H.; Nearing, M.A.; Liu, B.-Y. Potential effects of climate change on rainfall erosivity in the Yellow river basin of China. *Trans. ASAE* **2005**, *48*, 511–517. [[CrossRef](#)]
2. Chen, T.; Jiao, J.; Wang, H.; Zhao, C.; Lin, H. Progress in Research on Soil Erosion in Qinghai-Tibet Plateau. *Acta Pedol. Sin.* **2020**, *57*, 547–564. (In Chinese)
3. Wang, X.; Guo, Z.; Chang, C.; Wang, R.; Li, J.; Li, Q.; Qing, L. Spatiotemporal of soil wind erosion modules in the agro-pastoral ecotone of north China. *J. Desert Res.* **2020**, *40*, 12–22.
4. Hai, C.; Shi, P.; Liu, B.; Yan, P. Research status of wind and water double erosion and its main study content in future. *J. Soil Water Conserv.* **2002**, *16*, 50–56. (In Chinese)
5. Zhang, P.; Yao, W.; Liu, G.; Xiao, P. Research progress and prospects of complex soil erosion. *Trans. Chin. Soc. Agric. Eng.* **2019**, *35*, 154–161. (In Chinese)
6. Ma, Q.; Xiao, J.; Yao, Z.; Wei, M.; Wu, Q.; Hong, X. Spatio-temporal evolution of wind erosion climatic erosivity in the Alxa plateau during 1960–2017. *Sci. Geogr. Sin.* **2021**, *24*, 19–23.
7. Yue, S.; Yang, R.; Yan, Y.; Yang, zh.; Wang, D. Spatial and temporal variations of wind erosion climatic erosivity in the farming-pastoral zone of northern China. *Theor. Appl. Climatol.* **2019**, *135*, 1339–1348. [[CrossRef](#)]
8. Zhang, J.; Liu, Z.; Yang, M.; Zhang, F.; Wang, Y.; Deng, X. Soil erosion and its influence factors on a slope in the wind-water erosion crisscross region on the loess plateau. *J. Soil Water Conserv.* **2018**, *25*, 1–7. (In Chinese)
9. Song, Y.; Liu, L.; Yan, P. A review on complex erosion by wind and water research. *Acta Geogr. Sin.* **2006**, *1*, 77–88. (In Chinese) [[CrossRef](#)]
10. Zhang, Y.; Li, Z.; Zhang, X.; Niu, W.; Tang, S. Landform spatial distribution features of soil erosion in Dongliu valley of inner Mongolia. *J. Inn. Mong. Agric. Univ.* **2016**, *37*, 50–58. (In Chinese)
11. Xie, Y.; Yin, S.; Liu, B.; Nearing, M.; Zhao, Y. Models for estimating daily rainfall erosivity in China. *J. Hydrol.* **2016**, *535*, 547–558. [[CrossRef](#)]
12. Yang, H.; Wang, J.; Zou, X.; Shi, P. Progress and prospect of research on wind-water complex erosion. *J. Desert Res.* **2020**, *36*, 962–971. (In Chinese)
13. Yang, Y.; Zhao, R.; Shi, Z.; Viscarra Rossel, R.; Wang, D.; Liang, Z. Integrating multi-source data to improve water erosion mapping in Tibet, China. *Catena* **2018**, *169*, 31–45. [[CrossRef](#)]
14. Yue, T.; Yin, S.; Xie, Y.; Yu, B.; Liu, B. Rainfall erosivity mapping over mainland China based on high-density hourly rainfall records. *Earth Syst. Sci. Data* **2022**, *14*, 665–682. [[CrossRef](#)]
15. Yue, L.; Zhao, W.; Yan, X. Global rainfall erosivity changes between 1980 and 2017 based on an erosivity model using daily precipitation. *Catena* **2020**, *194*, 104768.
16. Wang, H.; Zhao, W.; Jia, L. Progress and prospect of soil water erosion research over past decade based on the bibliometrics analysis. *Sci. Soil Water Conserv.* **2021**, *25*, 1–7. (In Chinese)
17. Cui, B.; Zhang, Y.; Liu, L.; Xu, Z.; Wang, Z.; Gu, C.; Wei, B.; Gong, D. Spatialtemporal variation in rainfall erosivity and correlation with ENSO on the Tibetan plateau since 1971. *Environ. Res. Public Health* **2021**, *18*, 11054. [[CrossRef](#)]

18. Cheng, G.; Wu, T. Responses of permafrost to climate change and their environmental significance, Qinghai-Tibetan plateau. *J. Geophys. Res. Earth Surf.* **2007**, *112*, F02S03. [[CrossRef](#)]
19. Padulano, R.; Rianna, G.; Santini, M. Datasets and approaches for the estimation of rainfall erosivity over Italy: A comprehensive comparison study and a new method. *J. Hydrol. Reg. Stud.* **2021**, *34*, 100788. [[CrossRef](#)]
20. Liu, B.; Tao, H.; Song, C.; Guo, B.; Shi, Z.; Zhang, C.; Kong, B.; He, B. Temporal and spatial variations of rainfall erosivity in China during 1960 to 2009. *Geogr. Res.* **2013**, *32*, 245–256. (In Chinese)
21. Sadeghi, S.H.; Tavangar, S. Development of station models for estimation of rainfall erosivity factor in different timescales. *Nat. Hazards* **2015**, *77*, 429–443. [[CrossRef](#)]
22. Panagos, P.; Borrelli, P.; Poesen, J.; Ballabio, C.; Lugato, E.; Meusburger, K.; Montanarella, L.; Alewell, C. The new assessment of soil loss by water erosion in Europe. *Environ. Sci. Policy* **2015**, *54*, 438–447. [[CrossRef](#)]
23. Lin, H.; Zheng, S.; Wang, X. Soil erosion assessment based on the RUSLE model in the three-river headwater area. Qinghai-Tibetan plateau, China. *Acta Prataculturae Sin.* **2017**, *26*, 11–22. (In Chinese)
24. Zhang, W.; Xie, Y.; Liu, B. Rainfall erosivity estimation using daily rainfall amounts. *Sci. Geogr. Sin.* **2002**, *22*, 705–711. (In Chinese)
25. Chen, Y.; Xu, M.; Wang, Z.; Chen, W.; Lai, C. Reexamination of the Xie model and spatiotemporal variability in rainfall erosivity in mainland China from 1960 to 2018. *Catena* **2020**, *195*, 104837. [[CrossRef](#)]
26. Yin, S.; Xue, X.; Yue, T.; Xie, Y.; Gao, G. Spatiotemporal distribution and return period of rainfall erosivity in China. *Trans. Chin. Soc. Agric. Eng.* **2019**, *35*, 105–113. (In Chinese)
27. Gao, G.; Yin, S.; Chen, T.; Huang, D.; Wang, W. Spatiotemporal variation and cause analysis of rainfall erosivity in the Yangtze River Basin of China. *Trans. Chin. Soc. Agric. Eng.* **2022**, *38*, 84–92. (In Chinese)
28. Chen, S.; Dong, Y. A review of the research on wind erosion climatic erosivity. *J. Desert Res.* **2020**, *40*, 65–73. (In Chinese)
29. Allafta, H.; Opp, C. Soil erosion assessment using the RUSLE model, remote sensing, and GIS in the Shatt Al-Arab basin(Iraq-Iran). *Appl. Sci.* **2022**, *12*, 7776. [[CrossRef](#)]
30. Qi, D.; Li, X.; Su, W.; Zhou, W.; Xiao, H. Tendency of spatiotemporal evolution of wind erosion climatic erosivity in Qinghai province in recent 50 years. *Res. Soil Water Conserv.* **2019**, *26*, 23–30. (In Chinese)
31. Lou, J.; Wang, X.; Cai, D. Spatial and temporal variation of wind erosion climatic erosivity and its response to ENSO in the Otindag desert, China. *Atmosphere* **2019**, *10*, 614. [[CrossRef](#)]
32. Liu, J.; Wang, X.; Zhang, L.; Guo, Z.; Chang, C.; Du, H.; Wang, H.; Wang, R.; Li, J.; Li, Q. Regional potential wind erosion simulation using different models in the agro-pastoral ecotone of northern China. *Int. Environ. Res. Public Health* **2022**, *19*, 9538. [[CrossRef](#)] [[PubMed](#)]
33. Jia, L.; Gao, H.; Fan, B.; Li, Z. Spatiotemporal characteristic of water-wind erosion dynamics over Northern China. *Res. Soil Water Conserv.* **2017**, *4*, 19–23. (In Chinese)
34. Zhao, H.; Zhang, F.; Yu, Z.; Li, J. Spatiotemporal variation in soil degradation and economic damage caused by wind erosion in Northwest China. *J. Environ. Manag.* **2022**, *314*, 115121. [[CrossRef](#)] [[PubMed](#)]
35. Chepil, W.S.; Siddoway, F.H.; Armbrust, D.V. Climatic factor for estimating wind erodibility of farm fields. *J. Soil Conserv.* **1962**, *17*, 162–165.
36. FAO. *A Provisional Methodology for Soil Degradation Assessment*; Food and Agriculture Organization of the United Nations: Rome, Italy, 1979.
37. Guo, Z.; Shi, Y.; Huang, F.; Fan, X.; Huang, J. Landslide susceptibility zonation method based on C5.0 descision tree and K-means cluster algorithms to improve the efficiency of management. *Geosci. Front.* **2021**, *12*, 101249. [[CrossRef](#)]
38. Li, N.; Lu, H. Regionalization method for water resources utilization based on cluster analysis. *J. Shenyang Univ. Technol.* **2021**, *29*, 575–588. (In Chinese)
39. Rehman, S. Long-term wind speed analysis and detection of its trends using Mann–Kendall test and linear regression method. *Arab. J. Sci. Eng.* **2013**, *38*, 421–437. [[CrossRef](#)]
40. Xie, J.; Yu, Y.; Liu, C.; Ge, J. Characteristics of surface sensible heat flux over the Qinghai-Tibetan Plateau and its response to climate change. *Plateau Meteorol.* **2018**, *37*, 28–42. (In Chinese)
41. Zhang, L.; Wang, H.; Shi, X.; Li, D. Characteristics and Causes of surface sensible heat trend Transition in central and Eastern Qinghai-Xizang Plateau. *Plateau Meteorol.* **2020**, *39*, 912–924. (In Chinese)
42. Li, L.; Li, H.; Shen, H.; Liu, C.; Ma, Y.; Zhao, Y. The truth and inter-annual oscillation causes for climate change in the Qinghai-Tibet Plateau. *J. Glaciol. Geocryol.* **2018**, *40*, 1079–1089. (In Chinese)
43. Liu, Y.; Ma, Y.; Yang, Y.; Li, B.; Zhu, B. Research of the spatio-temporal variation characteristics of daytime and nighttime precipitation in the Qinghai plateau from 1961 to 2018. *J. Glaciol. Geocryol.* **2020**, *42*, 996–1006. (In Chinese)
44. Li, F.; Xue, W. Spatial and temporal variation of NDVI in different functional areas of Qinghai from 2000 to 2015. *Acta Agrestia Sin.* **2017**, *25*, 701–710. (In Chinese)
45. Zhao, H.; Li, X.; Zhao, D.; Xiao, R. Above ground biomass in grassland in Qinghai estimated from MODIS data and its influencing factor. *Acta Prataculturae Sin.* **2020**, *29*, 5–16. (In Chinese)
46. Qinghai Water Resources Department. Qinghai Bulletin of Soil and Water Conservation. 2005; p. 12. Available online: <http://www.doc88.com/p-6691320584305.html> (accessed on 22 August 2022).
47. Qinghai Water Resources Department. Qinghai Bulletin of Soil and Water Conservation. 2020; p. 12. Available online: <http://slj.haixi.gov.cn/info/1037/25916.html> (accessed on 22 August 2022).